Edge Extraction With an Anisotropic Vector Field Using Divergence Map

Giuliani Donatella *giulianidonatella@libero.it*
Scientifc-Didactic Polo of Rimini
University of Bologna
Via Angherà 22, Rimini, Italy

Abstract

The aim of this work is edge detection by a deformable contour procedure, using an external force field derived from an anisotropic flow, with different external and initial conditions. By evaluating the divergence of the force field, we have generated a divergence map associated with it in order to analyze the field convergence. As we know, divergence measures the intensity of convergence or divergence of a vector field at a given point, so by means level curves of the divergence contour map, we have automatically selected an initial contour for the deformation process. The initial curve must include areas from which the vector field diverges pushing it towards edges. Furthermore the divergence map brings out the presence of curves pointing to the most significant geometric parts of boundaries corresponding to high curvature values, in this way it will result better defined geometrical shape of the extracted object.

Keywords: Edge Extraction, Active Contours, Anisotropic Flow, GGVF

1. INTRODUCTION

Image segmentation and boundary extraction are diffusely handled topics of research in image processing. These problems have been dealt with in various forms [1], [2] [3], [4],[5],[6],[7] nevertheless the initial conditions and the ability to change the topology of the evolving curve are the main limitations for most of these methods. Edge detection may be realized by a deformable contour process with active contours or surfaces embedded within an image domain that move under the influence of internal and external forces [1],[6]. Internal forces, which are defined within the curve or surface itself, are designed to smooth the model during deformation. External forces, which are computed from image data, are used to move the model toward researched features in the image [8],[9],[10]. In this paper the external force field is derived from an anisotropic flow, in a more general framework respect to the GGVF [10],[11], in order to come to an overall view of the field flow, analyzed through its divergence values. A careful overview of divergence map, showing the divergence of the external force field, gives us the opportunity to circumscribe areas within which we can place an initial contour that may be subsequently deformed.

2. PRELIMINARIES

In the traditional parametric models an active contour or snake, expressed explicitly by parametric equations $\vec{x}(s) = (x(s), y(s)), \quad s \in [0,1]$, is defined within a given image *I(x,y)* and subjected to modifications under the action of forces, until the evolving curve fits well into the final contour [1],[7]. The final shape of the contour to be extracted will be such as to minimize an energy functional associated with it, so given:

$$E(\vec{x}(s)) = \int E_{Int}(\vec{x}(s)) + E_{Ext}(\vec{x}(s))ds \qquad (1)$$

the first term is the *internal energy* that expresses a priori knowledge of the model in relation to the degree of flexibility of an active contour:

$$E_{Int}(\vec{x}(s)) = \int \frac{1}{2}\left[\alpha(s)\cdot\left|\frac{d\vec{x}}{ds}\right|^2 + \beta(s)\cdot\left|\frac{d^2\vec{x}}{ds^2}\right|^2\right]ds \qquad (2)$$

the term $\alpha(s)$ controls the contour tension, while $\beta(s)$ regularises its rigidity. The second term $E_{Ext}(\vec{x}(s))$ represents the *external energy* related to a potential energy function $P(\vec{x}(s))$ deriving from the image *I(x,y),* whose local minima correspond to edges of the features to be extracted. By using a variational approach [12], the contour that minimizes the total energy must satisfy the Euler-Lagrange equation:

$$-\frac{d}{ds}\left(\alpha\frac{d\vec{x}}{ds}\right) + \frac{d^2}{ds^2}\left(\beta\frac{d^2\vec{x}}{ds^2}\right) + \nabla P = 0 \qquad (3)$$

where ∇ is the gradient operator. Through energy minimization we derive a resolution of a static problem. We could construct a deformable model able to create a geometrical shape that evolves over time, by introducing a time-variable parametric equation $\vec{x}(s,t) = (x(s,t), y(s,t))$. To this end, indicating with $\mu(s)$ and $\gamma(s)$ the density of mass and the damping coefficient respectively, instead of equation (3) we obtain:

$$\mu\frac{\partial^2\vec{x}}{\partial t^2} + \gamma\frac{\partial\vec{x}}{\partial t} - \frac{\partial}{\partial s}\left(\alpha\frac{\partial\vec{x}}{\partial s}\right) + \frac{\partial^2}{\partial s^2}\left(\beta\frac{\partial^2\vec{x}}{\partial s^2}\right) = -\nabla P \qquad (4)$$

The equilibrium is reached when internal and external forces are equal, this implies achieving a steady state in which time derivatives will become null.
When the solution $\vec{x}(s,t)$ of equation (4) stabilizes, we carry out the result of equation (3). Neglecting the inertial term and thus the second order derivatives, considering dumping, elasticity and rigidity as constant functions, the numerical solution of equation (4), can be reduced to that one of the dynamic equation:

$$\begin{cases} \gamma \dfrac{\partial \vec{x}(s,t)}{\partial t} = \alpha \dfrac{\partial^2 \vec{x}(s,t)}{\partial s^2} - \beta \dfrac{\partial^4 \vec{x}(s,t)}{\partial s^4} + \vec{F}_{Ext}(\vec{x}) \\ \vec{x}(s,0) = \vec{x}_0(s) \end{cases} \quad (5)$$

where $\vec{x}_0(s)$ is an initial contour. In order to reduce the sensitivity of this model to the initial conditions, edge extraction may be realized using a different class of external forces, the GGVF force field or Generalized Gradient Vector Flow [10],[11],[13],[14] obtained by solving a diffusion problem. In the GGVF contour generation, the external force field will be referred as:

$$\vec{F}_{Ext}^{GGVF} = \vec{v}(\vec{x}) \quad (6)$$

Using the calculus of variations [12], the GGVF force field $\vec{v}(x, y)$ can be found by solving the following diffusion equation:

$$\vec{v}_t = g(|\nabla f|) \cdot \nabla^2 \vec{v} - h(|\nabla f|) \cdot (\vec{v} - \nabla f) \quad (7)$$

where ∇^2 is the Laplacian operator, $\nabla f(x, y)$ is the gradient of the *edge map f(x,y),* derived from the gradient of brightness function *I*(x,y), that can be computed as $f(x, y) = |\nabla(I(x, y)|$ or using any other edge detector. The edge map gradient are vectors directed towards boundaries to detect with norms significantly different from zero in proximity of them. In equation (7) $g(|\nabla f|)$ and $h(|\nabla f|)$ are space varying weighting functions, being dependent on absolute gradient of edge map, generally not uniform. The function $g(|\nabla f|)$ will be monotonically non-increasing, since the vector field $\vec{v}(x, y)$ will be weakly variable far from edges to be extracted where image intensities are uniform. On the other hand, $h(|\nabla f|)$ should be monotonically non-decreasing, therefore, when $|\nabla f|$ is large, the vector field $\vec{v}(x, y)$ should have a trend nearly equal to ∇f .

The main shortcomings to be overcome in the generation of deformable contours are: 1) the initialization problem, i.e. the excessive sensitivity to shape and initial position of an initial curve 2) the weak convergence of models towards edges, especially in regions with highly variable concavities 3) the capture range, i.e. the size of area inside which an active contour can be initialized to be able achieving the desired boundary. We would like to explore a method that tries to overcome one of the main drawbacks for most of the approaches that were introduced until now: the initialization problem. The convergence of arbitrary initial contours for the GGVF leads only partially to the expected results, giving seemingly incomprehensible outcomes, as we can see in Fig.1a, Fig1b and Fig.2a, Fig2b for two test images. This paper is concerned with the problem of identifying automatically [15],[16],[17] an initial contour using the divergence of a force field derived from an anisotropic vector flow.

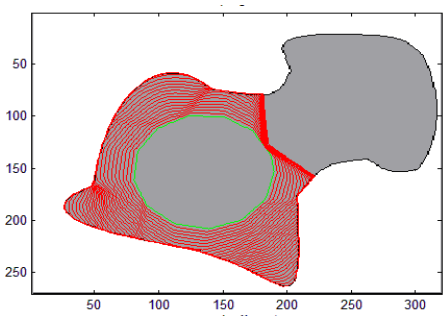

FIGURE 1a: Initialization problem

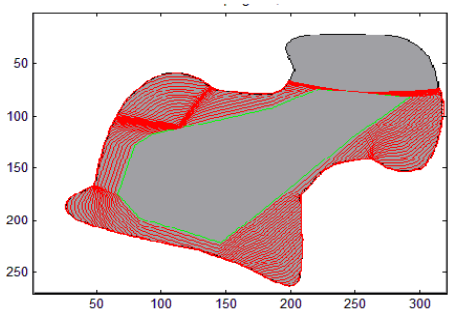

FIGURE 1b: Initialization problem

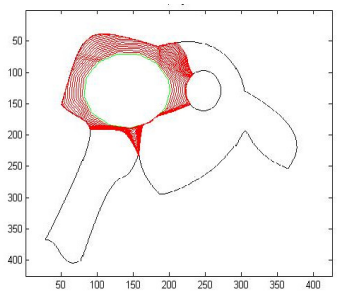

FIGURE 2a: Initialization problem

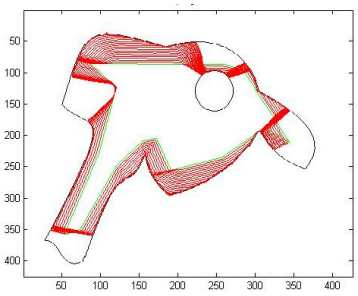

FIGURE 2b: Initialization problem

3. THE DIVERGENCE MAP OF AN ANISOTROPIC VECTOR FIELD

In this section we suggest a more general analysis of the diffusion process for an external force field. To this aim, we could see the solution of the GGVF equation (7) as the steady state of the following generalized parabolic equation:

$$\begin{cases} \vec{v}_t = div\left(g\left(\left|\nabla f\right|\right)\cdot\nabla\vec{v}\right)+\vec{F}(\vec{v}) \\ \vec{v}(x,\, y,0)=\vec{v}_0(x,\, y) \end{cases} \qquad (8)$$

where div is the divergence operator of the diffusion component and $\vec{F}(\vec{v})$ is a term generating an external force for the diffusion process of $\vec{v}(x,\, y)$, g(.) is the conduction coefficient that must be null or tend to zero at boundaries. So, in adiabatic condition hypothesis the vector flow is realized inside or outside the region. If the scalar-valued diffusivity function g(.) is monotonically non-increasing the diffusion has been stopping across the edges to be extracted. We obtain the GGVF field [11] if $\nabla g\left(\left|\nabla f\right|\right)\cdot\nabla\vec{v}=0$ $\vec{F}(\vec{v})=-h\left(\left|\nabla f\right|\right)\cdot(\vec{v}-\nabla f)$

$g\left(\left|\nabla f\right|\right)=e^{-\frac{\left|\nabla f\right|}{k}}$ $h\left(\left|\nabla f\right|\right)=1-g\left(\left|\nabla f\right|\right)$

with initial conditions $\vec{v}_0 = \nabla f$ and *k* as a constant positive value. If we consider an anisotropic flow for the vector field $\vec{v}(x, y)$ expressed as follows:

$$\begin{cases} \vec{v}_t = div\left(g\left(|\nabla f|\right) \cdot \nabla \vec{v}\right) \\ \vec{v}(x, y, 0) = \nabla f \end{cases} \quad (9)$$

where $\vec{F}(\vec{v}) = 0$, we carry out results rather similar to those of the GGVF field, given that the term $\vec{F}(\vec{v}) = -h(|\nabla f|) \cdot (\vec{v} - \nabla f)$ tends to zero whether near edges, for the chosen initial conditions, or far from them, since the function $h(|\nabla f|)$ is getting irrelevant, consequently the overall contribution of $\vec{F}(\vec{v})$ is not significant. But now considering the problem through the parabolic equation (9), we could interpret the process as a field flow from boundaries toward inside or outside without crossing edges and pointing to them because initially equal to the edge map gradient (Fig.3b). We could note from Fig.3a that the vector field can capture object boundaries from either sides. As we know, divergence is a measure of a field convergence or divergence at a given point by means signed scalar values. So if we compute the divergence of $\vec{v}(x, y)$, we would obtain negative values corresponding to object boundaries towards which the vector field converges, sinks of the flow, whereas positive values would define regions from which the field flow springs out, the flow sources.

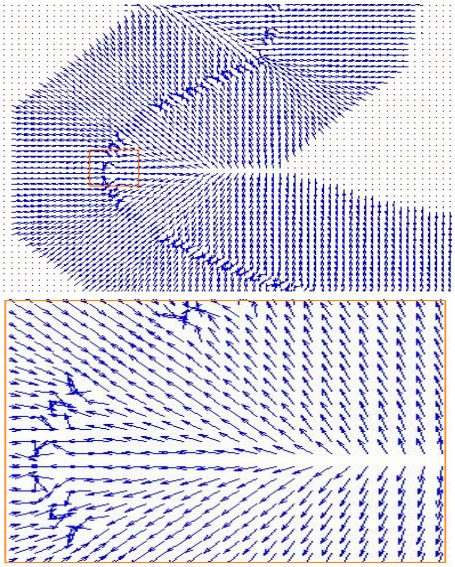

FIGURE 3a: The vector field $\vec{v}(x, y)$

FIGURE 3b: The vector field $\vec{v}(x, y)$

As a consequence, the analysis of divergence of the external force field $\vec{v}(x, y)$ may be very useful to feature detection, since it allows to demarcate regions from which the flow has been originated. Furthermore in correspondence of long and narrow boundary indentations, the field convergence towards opposite very near sides gives rise to zones of high positive divergence (Fig.3a,3b), hence divergence values may well highlight them. An efficient numerical scheme to resolve the anisotropic diffusion equation (9) may be that one proposed by Perona-Malik [18] and realized recurring to the 4-neighbors discretization of the Laplacian operator:

$$\vec{v}_{i,j}^{\,t+1} = \vec{v}_{i,j}^{\,t} + \lambda\left[g_N \nabla_N \vec{v}_{i,j}^{\,t} + g_S \nabla_S \vec{v}_{i,j}^{\,t} + g_E \nabla_E \vec{v}_{i,j}^{\,t} + g_W \nabla_W \vec{v}_{i,j}^{\,t}\right]$$
$$\nabla_N \vec{v}_{i,j} = \vec{v}_{i-1,j} - \vec{v}_{i,j}$$
$$\nabla_S \vec{v}_{i,j} = \vec{v}_{i+1,j} - \vec{v}_{i,j} \qquad (10)$$
$$\nabla_E \vec{v}_{i,j+1} = \vec{v}_{i,j+1} - \vec{v}_{i,j}$$
$$\nabla_W \vec{v}_{i,j} = \vec{v}_{i,j-1} - \vec{v}_{i,j}$$

with $\lambda = \frac{1}{4}$, and values of the edge-stopping function g(.) evaluated through a gradient approximation of $|\nabla f|$ along horizontal and vertical directions, such as:

$$g_N = g\left(\left|f_{i-1,j} - f_{i,j}\right|\right)$$
$$g_S = g\left(\left|f_{i+1,j} - f_{i,j}\right|\right)$$
$$g_E = g\left(\left|f_{i,j+1} - f_{i,j}\right|\right)$$
$$g_W = g\left(\left|f_{i,j-1} - f_{i,j}\right|\right)$$

The anisotropic vector field so obtained, from now on AVF, is partially shown in Fig.4a and Fig.4b for different numbers of time iterations, it results very similar to that one evaluated with the GGVF approach already seen. At first we could note that the size and the shape of capture range vary with the number of iterations performed in equation (9).

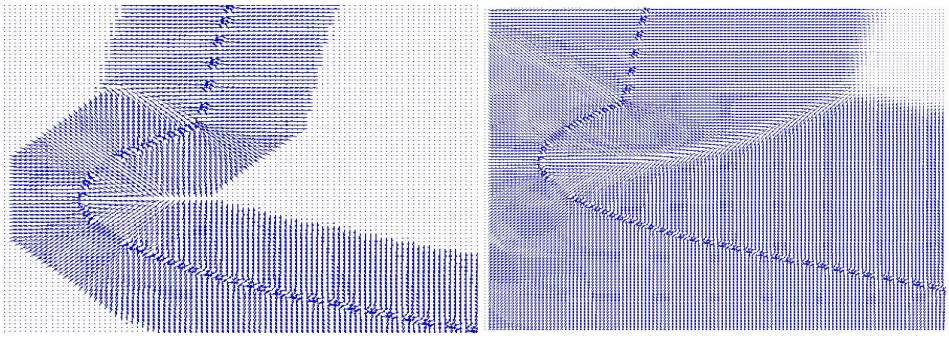

FIGURE 4a: AVF field from equation (9) after 20 iterations

FIGURE 4b: AVF field from equation (9) after 140 iterations

If now we consider equation (8) with an external force $\vec{F}(\vec{v})$ significantly different from zero, the convergence of $\vec{v}(x, y)$ to the steady state will result faster than the GGVF solution. By using the diffusion equation:

$$\begin{cases} \vec{v}_t = div\left(g\left(|\nabla f|\right)\cdot\nabla\vec{v}\right)+\vec{F}(\vec{v}) \\ \vec{v}(x, y, 0)=\nabla f \end{cases} \qquad (11)$$

with, for example, an the external force $\vec{F}(\vec{v})=g\left(|\nabla f|\right)\cdot(\vec{v}-\nabla f)$ we will be able to speed up the convergence process, because $\vec{F}(\vec{v})$ is approximately null near edges but increases as moving away from them. This implies an extension of capture range for an equal number of time iterations. In Fig.5a and Fig.5b we could compare the AVF field derived from equation (11) with GGVF field obtained through equation (7). With the same number of iterations it has been realized an increase of capture range, the region inside of which must be placed any initial contour. Consequently the evaluation of the AVF vector field will be less time consuming respect to the GGVF because we could choose a reduced number of iterations to achieve similar results. In Fig.5c and Fig.5d we have compared the results obtained by AVF field with those of GGVF using the same number of iterations (in the case in point 80) and the same initial polygonal. Recurring to 120 iterations to research the solution of equation (7), the GGVF field has been able to detect edges completely.

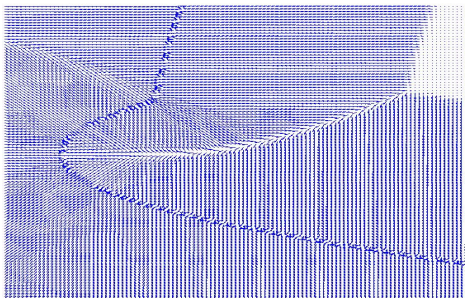

FIGURE 5a: AVF field from equation (11) after 80 iterations

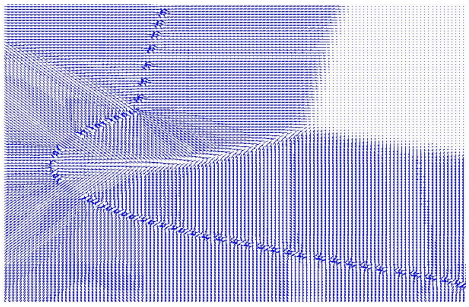

FIGURE 5b: GGVF field from equation (7) after 80 iterations

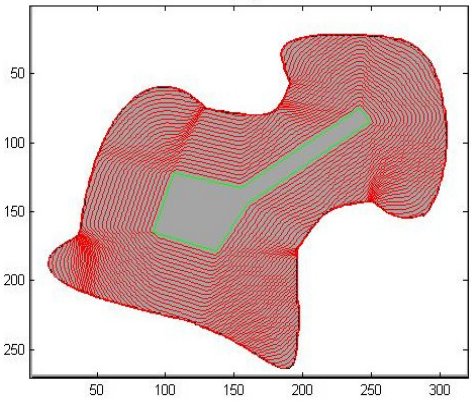

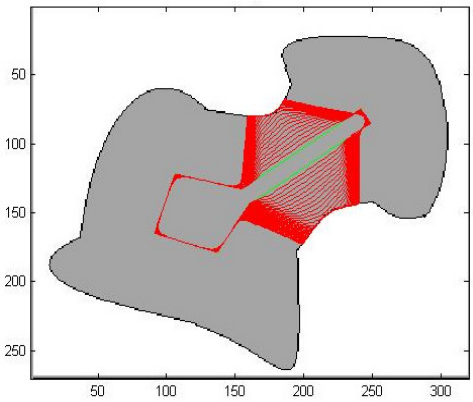

FIGURE 5c: AVF field from equation (11) **FIGURE 5d:** GGVF field from equation (7) with the same initial contour after 80 iterations

As an alternative approach we could evaluate the vector field $\vec{v}(x, y)$ using diffusion equation (11) but recurring to different external forces and initial conditions, so we have:

$$\begin{cases} \vec{v}_t = div\left(g\left(|\nabla f|\right)\cdot\nabla\vec{v}\right)+\vec{F}\left(\vec{v}\right) \\ \vec{v}(x, y,0)=0 \end{cases} \qquad (12)$$

where now $\vec{F}\left(\vec{v}\right)$ is an external attractive force directed towards edges, for example of the type $\vec{F}(\vec{v})=h(|\nabla f|)\cdot(\vec{v}-\nabla f)$ that stops acting when the vector field, initially null everywhere, tends to the edge map gradient. Again, by a comparison between the AVF field generated with equation (12) and the GGVF field after the same number of iterations, we could verify an acceleration of the convergence process (Fig.6a,6b). Therefore the area, within which the field is able to act on a deformable initial contour pushing it towards edges, is larger with the AVF field of equation (12) than GGVF. As a consequence, we need a smaller number of iterations to obtain a vector field as effective as the GGVF.

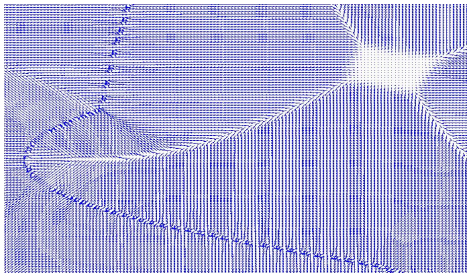

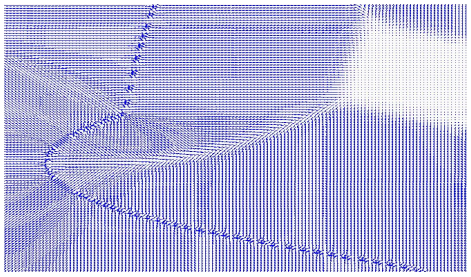

FIGURE 6a: AVF field from equation (12) after 140 iterations

FIGURE 6b: GGVF field from equation (7) after 140 iterations

After these considerations, we may suggest a method to generate automatically an initial curve, that could be able to adequately reconstruct the final contour. Indeed the effects due to initialization problem and capture range extension are reduced using the divergence map of the normalized force field, defined as:

$$I_D(x, y, t) = div\left(\frac{\vec{v}(x, y, t)}{|\vec{v}(x, y, t)|}\right)$$

In the following figures it has been shown divergence maps corresponding to vector fields resulted as numerical solutions of equation (9) at different times t, i.e. for different numbers of iterations, referred to the first test image (Fig.7a,7b,7c,7d) and to the second one (Fig.8a,8b,8c,8d) respectively:

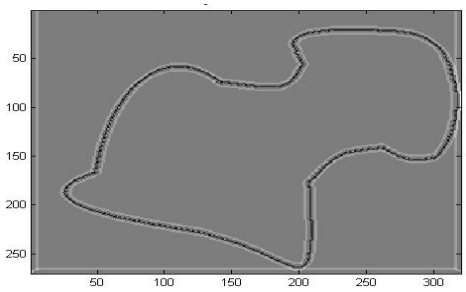

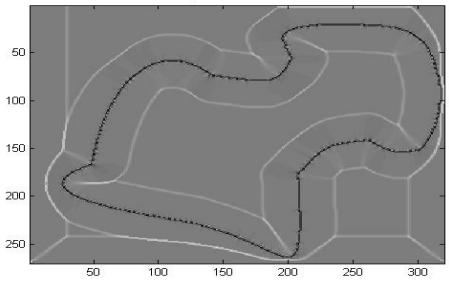

FIGURE 7a: Divergence Map of AVF from equation (9) after 0 iterations

FIGURE 7b: Divergence Map of AVF from equation (9) after 30 iterations

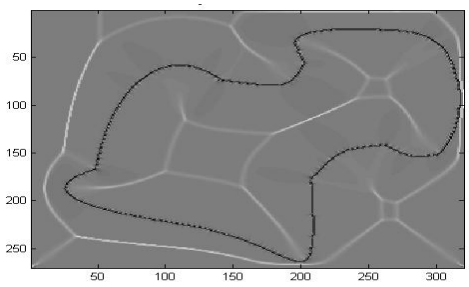

FIGURE 7c: Divergence Map of AVF from equation (9) after 100 iterations

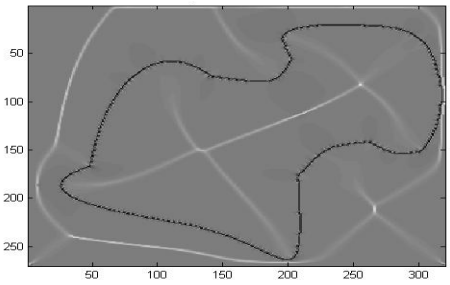

FIGURE 7d: Divergence Map of AVF from equation (9) after 240 iterations

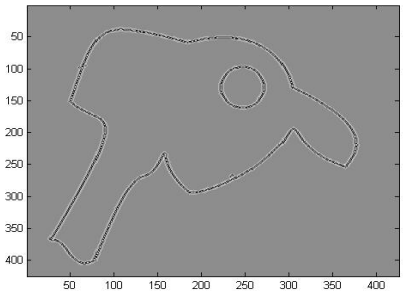

FIGURE 8a: Divergence Map of AVF from equation (9) after 0 iterations

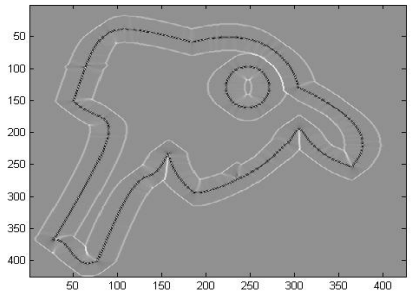

FIGURE 8b: Divergence Map of AVF from equation (9) after 20 iterations

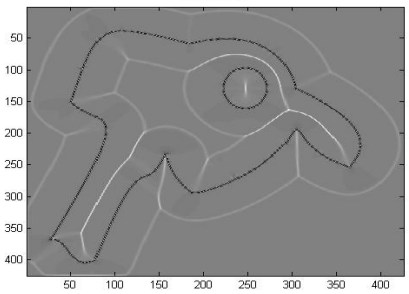

FIGURE 8c: Divergence Map of AVF from equation (9) after 80 iterations

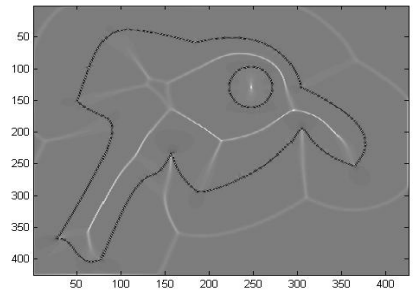

FIGURE 8b: Divergence Map of AVF from equation (9) after 200 iterations

By an accurate analysis of the shown figures, we may point out that each divergence map is characterized by a gray background with divergence values near zero, dark curves with negative divergence corresponding to edges, towards which the vector field converges, and a system of light curves with positive values, defining regions from which the vector field comes out. These regions are varying with the number of iterations after which the flow process has been interrupted.

The zones between opposite values of divergence define the capture range size. Moreover, by increasing the iteration number, the sides of areas that delimit parts of image inside which the field is null, collapse each other, especially in conjunction with deep and narrow concavities (see Fig.8b and Fig.8c). Thereby these curves, corresponding to positive divergence values, remain as traces of those edge sections with high curvatures and concur in forming the skeleton of the figure, as we can see in Fig.7d after 240 iterations for the solution of equation (9) or in Fig.9 only after 120 iterations for the solution of equation (11). In Fig.9 and Fig.10 we may compare divergence maps for AVF field evaluated by equation (11) and GGVF field respectively.

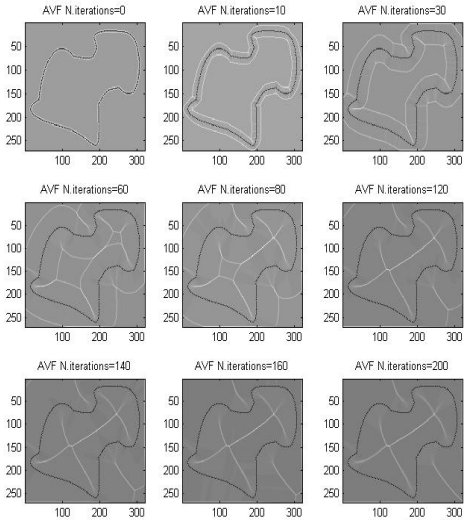

FIGURE 9: Divergence Maps of AVF field from equation (11) for different iteration numbers

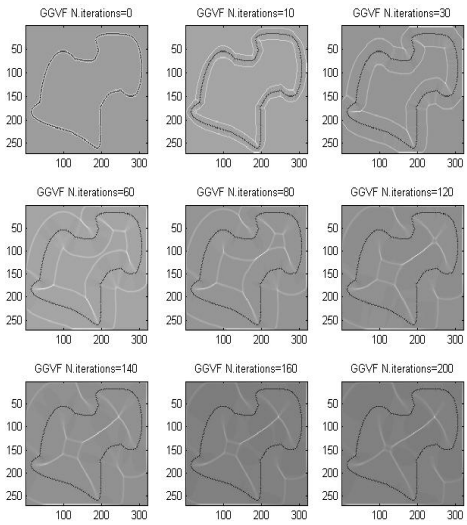

FIGURE 10: Divergence Maps of GGVF for different iteration numbers

As a consequence shape and position of any initial contour also depends on the number of iterations performed in the numerical resolution. We have to take into account boundaries of areas with positive divergence, because within them the vector field is null, so the sections of an evolving curve remain entrapped in their interiors, as we can see in Fig.11a, where an arbitrary initial contour is superimposed to the divergence map of our image.

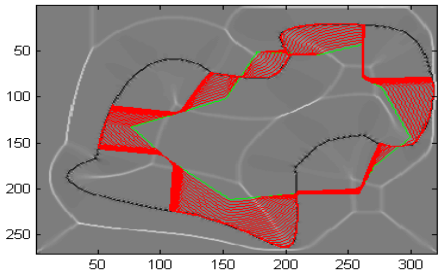

FIGURE 11a: Divergence Map of GGVF field with an arbitrary initial contour after 80 iterations

If we now review the results shown in Fig.5c and Fig.5d realized using AVF field and GGVF field respectively, after 80 iterations and we superimpose the initial polygonal with the corresponding divergence maps, we are able to understand the anomalous shape of the extracted edges of Fig.5d, apparently incomprehensible. Some portions of the initial contour fall within the areas where the GGVF field is null, thereby those traits remain trapped inside them (see Fig.11c). Instead after 120 iterations, the capture range of the GGVF field is become more extended, so the evolving curve converges to right results

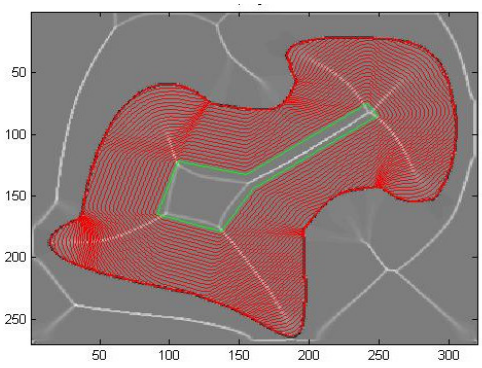

FIGURE 11b: Divergence Map of AVF field field from equation (11) after 80 iterations

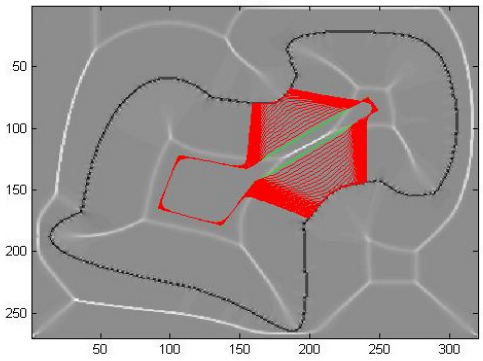

FIGURE 11c: Divergence Map of GGVF from equation (7) after 80 iterations

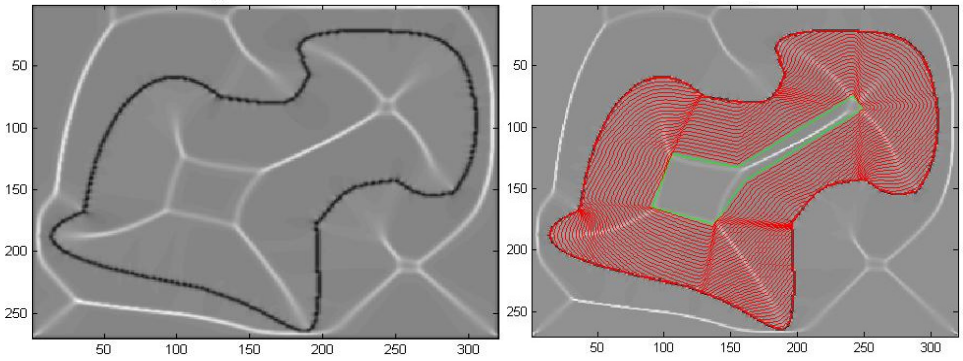

FIGURE 11d: Divergence Map and active contour with GGVF field after 120 iterations

We would remember that divergence will be zero either when the field is null or when the inward and the outward flux are equal. In the divergence map relative to the second test image, composed by two disjoint boundaries, we may well see two closed curves corresponding to positive divergence values. Within the first curve the field is zero, instead inside the second, divergence values are near zero because the flux is null, whereas the vector field is rather uniform and changes its direction converging to the inner circle, as we can see in Fig.12a. Then the traits of an initial contour that fall inside this region are pushed towards the inner circle rather than the outer edge (Fig.12b,112c).

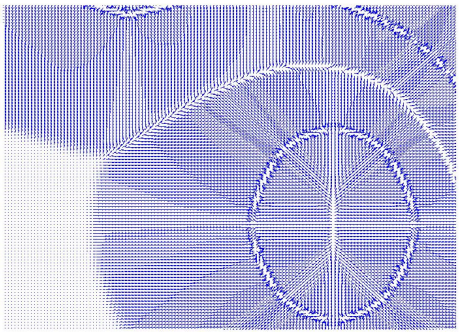

FIGURE 12a: AVF field after 80 iterations

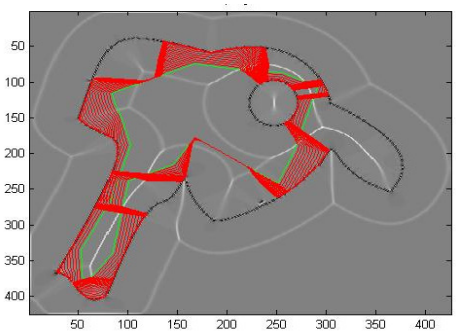

FIGURE 12b: Divergence Map of AVF field with an arbitrary initial contour

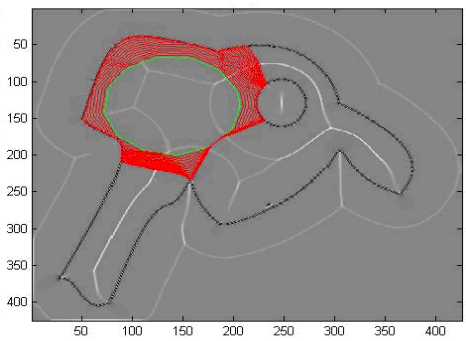

FIGURE 12c: Divergence Map of AVF field with an arbitrary initial contour

Thereby it results much easier to understand the anomalous behaviour in the convergence of each polygonal sections of Fig.11a, Fig.11b, Fig.11c or Fig.12b, Fig.12c using maps of divergence associated with the GGVF or AVF field. The traits of an initial contour are pushed along the field lines that, according to the Divergence Theorem, start at sources, i.e. areas of positive divergence, and end at sinks with negative divergence. In addition we would like to make some observations about the capture range extension. Looking closely at the divergence map, we could note that the area enclosed between the external or internal curve with positive divergence, and the curve of negative divergence, corresponding to the object edge, delimits the capture range. As we may well see in Fig.7a, 7b, 7c, 7d and in Fig.8a, 8b, 8c, 8d, shape and size of this area are varying with the number of iterations chosen. So we may conclude that divergence map, at any given time, is strictly related to the initialization problem and the capture range, because it allow us to clearly distinguish between sources and sinks for our image, enabling us to properly place an initial curve, as shown in Fig.13. Accordingly we suggest to generate a contour map of the field divergence in order to visualize it through level sets, i.e. the set of points in the image domain where divergence is constant. In this way we could automatically extract an appropriate initial contour using level curves corresponding to high divergence values.

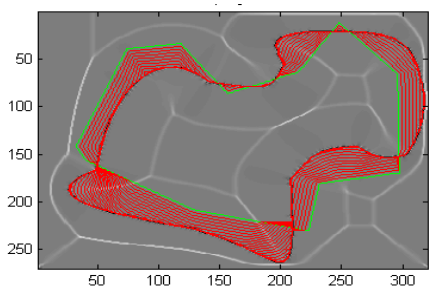

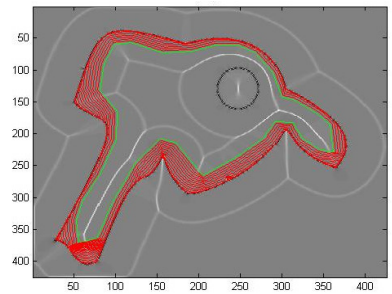

FIGURE13: Divergence Map with initial contours converging towards edges to detect

Given an image *I(x,y)*, it has been carried out $\vec{v}(x, y)$ resolving numerically equation (11). After evaluating its divergence map $I_D : D \subset R^2 \to C$ in the gray colour space C = [0;255], it has been generated a contour map concerning to it (Fig.14, Fig.15) and subsequently it has been selected as initial contour the level curve of intensity 153 for the two test images. In this way the chosen curve certainly encloses source areas from which the field diverges, pushing the active contour towards object edges. As we can see from Fig.16 to Fig.19, edges have been extracted correctly, establishing a quite good effectiveness of the proposed approach.

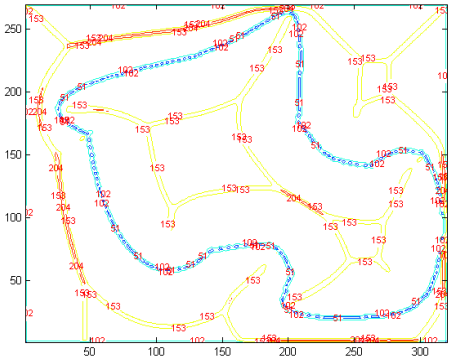

FIGURE 14: Level curves of Divergence Map

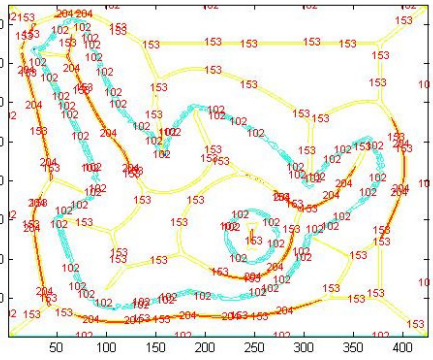

FIGURE15: Level curves of Divergence Map

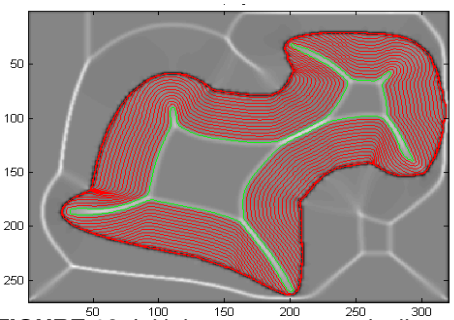

FIGURE.16: Initial contour automatically selected

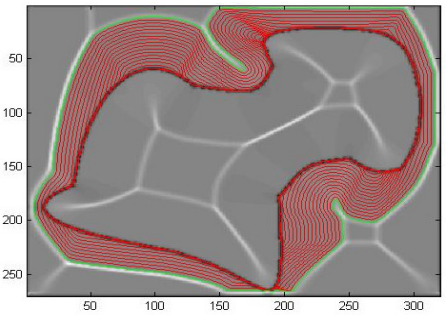

FIGURE.17: Initial contour automatically selected

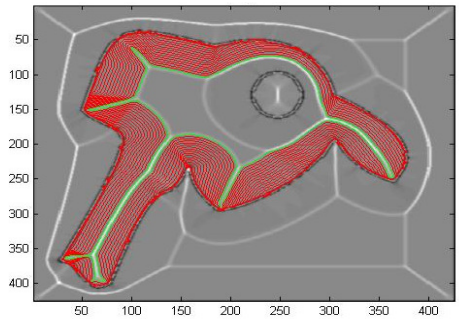

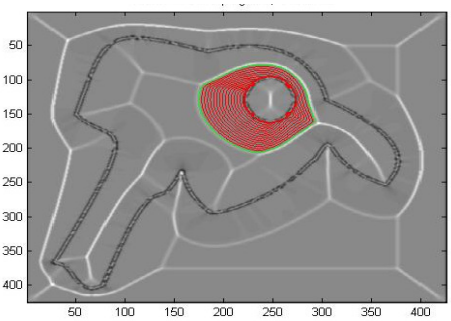

FIGURE. 18: Initial contour automatically selected **FIGURE.19**: Initial contour automatically selected

We have used real images for the validation of the proposed framework and promising experimental results were obtained with Gray Matter images derived from a data set of patients affected by Alzheimer disease (Fig.20) and subjects of a control group. This model doesn't require the user to input manually an initial curve close to the edges, that may be fastidious to do for an application dealing with a large number of images.

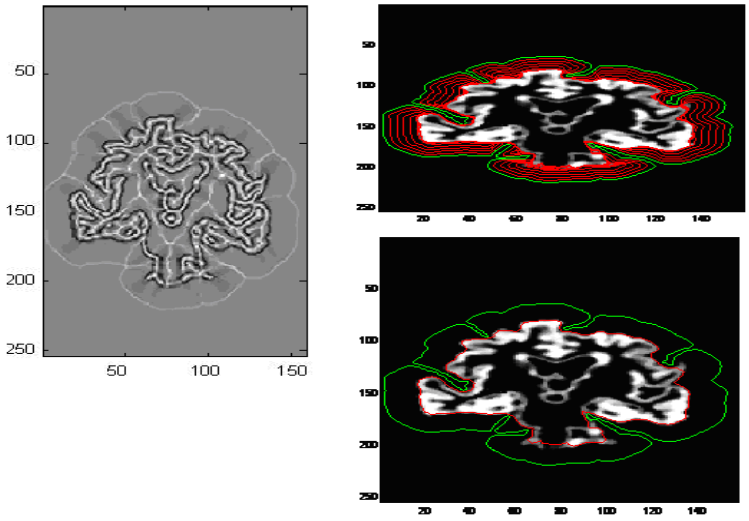

FIGURE 20: Initial contour automatically selected for a GM image after 10 Iterations

4. CONCLUSIONS

In this work, we have analyzed edge extraction by a deformable contour procedure, using an external force field derived from an anisotropic vector flow, with different diffusion equations and initial conditions. We have suggested a new

approach to overcome some limitations of traditional parametric snakes, specially regarding to the initialization problem. The external force field, resolution of an anisotropic diffusion problem, should be considered in relation to its divergence map, because the source areas, from which the vector field diverges pushing the deformable initial contour towards the edges to detect, are well defined and recognizable in it. We have observed that only if source areas are completely included inside the initial contour, the edge detection will turn out well. Moreover we have proposed as automatic initialization procedure the use of level curves of divergence contour map, in such a way it doesn't be required a specification of an initial curve by the user.

ACKNOWLEDGMENT

I sincerely would like to thank Prof. Naldi Giovanni (Department of Mathematics "Federigo Enriques", University of Milan – Italy) for the helpful contribution given for this study.

REFERENCES

[1] M. Kass, A. Witkin, D. Terzopoulos, " Snakes: active contour models" , Int. Jour. Comp. Vision, Vol. I, N.4, 1988, pp 321-331

[2] T. Mc Inerney, D. Terzopoulos, "T-snakes:Topology adaptive snakes" , Medical Image Analysis,4,2000,pp. 73-91.

[3] J. Liang,T.Mc Inerney, D. Terzopoulos, "United Snakes" , Medical Image Analysis,10,2006pp. 215-233

[4] S.J. Osher, J.A. Sethian, "Fronts propagating with curvature dependent speed: algorithms based on Hamilton-Jacobi formulations", J. of Computational Physics, 79, 1988, pp 12-49

[5] S.J. Osher, R.P. Fedkiw, "Level set methods: an overview and some recent results", J. of Computational Physics, 169, 2001, pp 463-502

[6] C. Xu, L.J. Prince, "Snakes ,shapes, and gradient vector flow", IEEE Trans. on Image Processing, 7, 1998

[7] C. Xu, A. Yezzi, and J. Prince, "On the Relationship between Parametric and Geometric Active Contours," Proc. Asilomar Conf. Signals, Systems, and Computers, pp. 483-489, 2000.

[8] B. Li, T.A Scott, "Active contour external force using vector field convolution for image segmentation",. IEEE Transactions on Image Processing, 16, 2007, pp.2096-2106

[9] A. Kovács, T. Szirányi, "Improved force field for vector field convolution method",
ICIP IEEE 2011, pp. 2909-2912.

[10] C. Xu, L.J. Prince, “Gradient Vector Flow: a New External Force for Snakes”, IEEE Proc. Conf. on Comp. Vis. Patt. Recogn., CVPR’97

[11] C. Xu, L.J. Prince, “Generalized gradient vector flow external forces for active contours”, Signal Proc., an Intern. Journal, 71, 1998

[12] R. Courant,D. Hilbert, “Methods of Mathematical Physics”, Vol I, Ed. Interscience, New York,1953

[13] J. Cheng, W.F. Say, “Dynamic Directional Gradient Vector Flow for Snakes”, IEEE Trans. on Image Processing, 15, 2006

[14] N. Paragios, O. Mellina-Gottardo, V. Ramesh, “Gradient Vector Flow Fast Geometric Active Contours”, IEEE Trans. on Pattern Analysis and Machine Intelligence, 26, 2004

[15] C. Li, J. Li, M.D. Fox, “Segmentation of Edge Preserving Gradient Vector Flow: an Approach Toward Automatically Initializing and Splitting of Snakes”, IEEE Proc. Conf. on Comp. Vis. Patt. Recogn., CVPR’05

[16] C. Tauber, H. Batiata, A. Ayache, “A Robust Active Initialization and Gradient Vector Flow for Ultrasound Image Segmentation”, MVA2005 IAPR Conference on Machine Vision Applications, 2005

[17] F. Yabin, L. Caixia, Z. Bingsen, P. Zhenkuan, “An Improved Algorithm of Contour Initialization in Active Contour Model”,Image and Graphics, ICIG 2007

[18] P. Perona, J. Malik, “Scale-space and edge detection using anisotropic diffusion” IEEE Trans. on Pattern Analysis and Machine Intelligence, 12, 1990